British Journal of Applied Science & Technology
5(2): 198-209, 2015, Article no.BJAST.2015.019
ISSN: 2231-0843

SCIENCEDOMAIN *international*
www.sciencedomain.org

Synthesis and Study of Corrosion Protection Efficiency of Silica Nanoparticles on Aluminium

Pradip Kr. Ghosh[1], Bikash Mandal[1], Susanta Ghosh[2] and I. Basumallick[1*]

[1]Electrochemistry Laboratory, Department of Chemistry, Visva-Bharati University, Santiniketan-731235, India.
[2]Electrochemistry Laboratory, Integrated Science Education and Research Centre, Visva-Bharati University, Santiniketan-731235, India.

Authors' contributions

This work was carried out in collaboration between all authors. All the authors read and approved the final manuscript.

Article Information

DOI: 10.9734/BJAST/2015/13318
Editor(s):
(1) Deepak Pudasainee, Karlsruhe Institute of Technology, Institute for Technical Chemistry (ITC), Germany.
Reviewers:
(1) Anonymous, Universiti Kebangsaan Malaysia, Malaysia.
(2) Benedict Iserom Ita, Chemistry, Covenant University, Ota, Ogun State, Nigeria.
(3) Anonymous, Middle East Technical University, Ankara, Turkey.
(4) Anonymous, University of Málaga, Málaga, Spain.
Complete Peer review History: http://www.sciencedomain.org/review-history.php?iid=713&id=5&aid=6581

Original Research Article

Received 12th August 2014
Accepted 8th October 2014
Published 22nd October 2014

ABSTRACT

Monodispersed silica nanoparticles (SNPs) were synthesized by cost effective aqueous-ethanolic route. The particle size was controlled by optimizing the synthetic conditions. The synthesized different size SNPs were used to study the corrosion protection efficiency on aluminium (Al) in alkaline medium by weight loss, Potentiodynamic polarization and surface morphology examination methods. It was found that SNPs with smaller particle sizes showed better protection efficiency compared to those of larger particles. The results were explained in terms of effective surface coverage by smaller sized SNPs.

Keywords: Silica nanoparticles; al corrosion protection; weight loss studies; E_{corr}; I_{corr}.

**Corresponding author: E-mail: ibasumallick@yahoo.co.uk;*

1. INTRODUCTION

Corrosion study has been an extremely significant issue since age old uses of metal objects [1]. The study of metal corrosion is not only of great academic interest but also related to tremendous economic importance. Aluminium (Al), the third most abundant metal on earth, is an important material for many applications including aviation, automobiles and household appliances. A good electrical, thermal conductivity, low density and high ductility properties of Al find various applications such as interconnects, electrodes in electronic devices and integrated circuits [2]. Aluminium gradually forms a natural, inert, and protective oxide layer under the atmospheric conditions which exhibits resistance to general corrosion. However, it is influenced to localized pitting corrosion, due to inter metallic inclusion which leads to exfoliation corrosion [3].

Al-air batteries are low cost, high power and energy densities comprises of Al anode and NaOH solution as electrolyte [4]. However, these batteries are not commercially used due to corrosion problem in alkaline medium. In alkaline medium, Al undergoes corrosion by forming a non conducting oxide film and gives off hydrogen gas which leads to sharp reduction of the anodic efficiency. Both these factors significantly reduce the efficiency of battery reactions [5]. Due to these corrosion problems, development of Al-air batteries facing challenges. Thus, Al corrosion inhibition has been extensively studied by various researchers using acidic and alkaline medium [6-8].

Hexa-valent chromium compounds have been found as the most effective corrosion protective materials for Al [6]. However, the use of chromates and other chromium-containing compounds are banned worldwide because of its toxic and carcinogenic effect [7]. Moreover, it is reported that inorganic inhibitors like phosphates, borates, tungstates, molybdates and arsenates have also found effective in the forming anti-corrosive coatings onto Al surface [8]. But the toxic effect of these inorganic inhibitors is a major disadvantage, which has come under severe criticism. These call for further research on development of an environmentally friendly, effective, economical and non-hazardous corrosion inhibitor.

Silica (SiO_2) is an environment friendly, low cost and nontoxic compound which shows excellent corrosion inhibition properties on metal due to the interaction between metal and dense -O-Si-O-Si-O- network [9-15]. However, the applications of macro silica particles onto metals create micro cracks on the metal surfaces. As a result, the penetration of aggressive species toward the metallic surface occurs. This issue may overcome with the application of nanoparticles as corrosion inhibitor on to metal surfaces [16-19].

Silica nanoparticles (SNPs) have been synthesized applying several techniques such as sol-gel process [20-22], microemulsion [23-25], oxidation of tetra ethoxy silane (TEOS) in the bench-scale diffusion flame reactor [26], an interdigital micromixer and a batch reactor [27]. Recently mesoporous silica nanoparticles for encapsulation for water insoluble drugs were obtained using supercritical carbon dioxide [28].

The current study is focused on synthesis of different sizes SNPs by chemical method from tetra-ethoxy silane (TEOS) and ethanol (C_2H_5OH) in the presence of 25% ammonia solution as catalyst at 303 K [29]. Particle sizes are controlled using different concentrations of TEOS keeping other parameters unchanged. The study is further extended by comparing the effect of various particle sized SNPs on Al corrosion in 0.1 M NaOH solution using weight loss, potentiodynamic polarization studies and surface characterization techniques.

2. MATERIALS AND METHODS

2.1 Reagents Used

Tetraethoxy Silane (TEOS) (Himedia, India, 98.0%), ethanol, ammonium solution (Merck, India, 25%), and NaOH (Merck, AR grade) were used without any further purification.

2.2 Synthesis of SNPs

The SNPs were synthesized by hydrolysis of TEOS by ammonia solution in ethanol medium. The concentrations of TEOS were varied for obtaining three different sizes of SNPs. SNPs were synthesized by the following procedure at 303 K.

First, 25 µl TEOS, 5 ml distilled water and 9 ml ethanol were mixed with constant stirring for 20 min. The solution was taken in a test tube and subjected to sonication for 30 min, followed by

drop wise addition of 5 ml ammonia solution. Sonication was further continued for 60 min to get a white turbid suspension. The turbid suspension was centrifuged at 12,000 rpm for 30 min to collect SNPs. The sample was marked as no. 1. For another two samples, marked as no.2 and no. 3, we used 0.2 ml and 0.5 ml TEOS solutions for the preparation.

2.3 Characterization of SNPs

SNPs were characterized by UV-Visible spectroscopy (PerkinElmer UV/VIS spectrometer Lambda 35), Fourier Transform Infrared Spectroscopy (FTIR, 8400S PC, Shimadzu, Japan), Powder X-Ray Diffraction (XRD, Ultima IV, Rigaku, Japan, CuKα, λ= 1.5406Å), Surface Area Electron diffraction (SAED, JEM 2100, JEOL), Transmission Electron Microscopy (TEM, JEM 2100, JEOL, Japan) and Energy Dispersive Spectroscopy (EDX, JEM 2100, JEOL).

The UV-VIS spectra analysis was performed by dispersing sample 1, 2 and 3 in 0.1 M NaOH solution for the entire studies. Particle sizes of SNPs were measured by TEM images. Three different sizes of SNPs samples were suspended in acetone medium for 60 min. Carbon coated copper grids were used to transfer a droplet of each suspended sample. The samples were allowed to dry for 24 hours and TEM images were taken at a number of random positions on the grid. EDX studies were carried out using carbon coated copper grid for assuring the presence of elements in prepared samples.

Weight loss of Al surface was determined at 303 K in the absence and presence of SNPs in 0.1 M NaOH solution. The Al foils (130 mg) having dimension 1 cm × 1 cm × 0.1 cm were suspended in 50 ml beakers containing 20 ml of each solution. The foils were retrieved at 5 h interval, progressively for 25 h. The foils were further washed by immersion in double distilled water and acetone. At the end of the test the foils were carefully washed in double distilled water and acetone to quench further corrosion. The foils were dried and weighed. The experiments were carried out in triplicate and the mean values were reported. The corrosion rate (C_{rate}) of Al was calculated using the relation:

$$C_{rate} = \Delta m / St \quad \text{..... (1)}$$

Where, C_{rate} is the corrosion rate of Al (mg cm^{-2} h^{-1}); Δm is the corrosion weight loss of Al (mg); S is the surface area of Al foils (cm^2); and t is the time of exposure in hour, respectively. The percentage corrosion inhibition efficiency (IE_W %) was calculated using the following equations:

$$IE_W\ \% = 100 \times [1-(C_{rate} / C^0_{rate})] \quad \text{..... (2)}$$

Where, C^0_{rate} and C_{rate} are the corrosion rates of Al in 0.1 M NaOH in the absence and presence of three SNPs samples, respectively.

Potentiodynamic polarization studies were carried out for measuring the corrosion potential (E_{corr}), corrosion current (I_{corr}), Tafel cathodic slopes (β_c), Tafel anodic slope (β_a) of Al in 0.1 M NaOH solution in the absence and presence of three samples of SNPs using potentiostat-galvanostat (Versastat II, PAR) at 303 K. The corrosion protection efficiency was computed from those data. The measurements were performed by exposing a high purity Al rod (Johnson, Matthey, UK, 99.9%) of area 3.5 cm^2 as working electrode, the platinum metal was used as counter electrode and saturated Calomel electrode (SCE) as reference electrode. The exposed surface of Al was polished with silicon carbide abrasive paper, washed with distilled acetone and dried in warm air. Prior to each experiment the working electrode was kept on open circuit conditions in the electrolyte for 30 minutes to attain equilibrium. The polarization measurements were carried out over a potential from -0.25 V to +0.25 V vs. SCE with respect to the open circuit potential at a sweep rate 0.5 mVs^{-1}. The linear Tafel segments of anodic and cathodic curves were extrapolated to obtain the I_{corr} values. The percentage corrosion protection efficiency (IE_T %) was calculated by using the following equation,

$$IE_T\ \% = [1 - (I_{corr} / I^0_{corr})] \times 100 \quad \text{..... (3)}$$

Where, I^0_{corr} and I_{corr} were the corrosion current densities of Al in 0.1 M NaOH in the absence and presence of SNPs samples respectively.

The surface morphology of Al in the absence and presence of sample 1 and 3 in 0.1 M NaOH solution were analyzed by FE-SEM instrument (ZEISS, SUPRA 55 VP).

3. RESULTS AND DISCUSSION

The UV-Visible spectra of three samples of SNPs in 0.1 M NaOH solution in the range of 400-700 nm are presented in Fig. 1. The patterns of all spectra were found to be similar and the absorption maximums were obtained at 539, 541

and 543 nm for samples 1, 2 and 3, respectively. A slight variation in wavelength is observed which may be attributed to different size of SNPs. With increasing size of SNPs, the absorption maxima show red shifted. Depending on band gap energy, the different absorption intensities typically characterize the interaction between particles and predict the variation in sizes of the particles [29]. Therefore, it is indicated from the UV-Vis studies that the particles size gradually increases from samples 1 to 3.

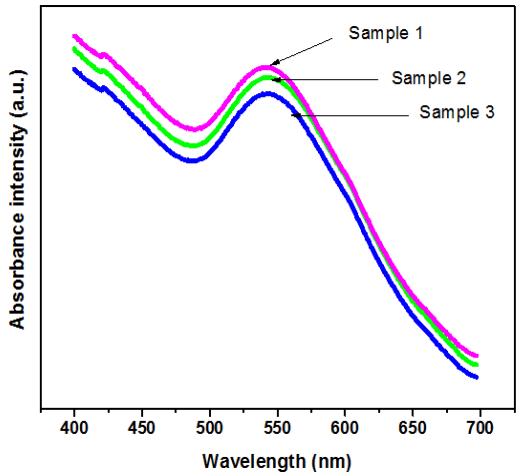

Fig. 1. UV-VIS spectra of sample 1, 2 and 3 in 0.1 M NaOH solution

The FTIR spectra of three SNPs samples are shown in Fig. 2 (A)-(C). The broad and strong absorption bands at 3200–3400 cm^{-1} are the signatures of water and silanol O–H groups [30,31]. SNPs can absorb water molecules from atmospheric air as reported recently [32]. The bands at around 1180-1200 cm^{-1} are due to the C-H rocking mode of $SiOCH_2CH_3$ [30–33]. Finally, the peaks around 1100–1049 cm^{-1} are due to asymmetric stretching of Si-O (Si–O–Si) [30–34], while 800-810 cm^{-1} bands may be considered for the bending vibration of Si-O [34]. Hence, the FTIR analysis confirmed the formation of SNPs and hygroscopic nature of the samples.

The powder XRD patterns shown in Fig. 3 of SNPs material comprise of two peaks; one broad peak around 23°may be due to the formation of silica glass like nanoparticles and other relatively narrow peak at 49º which may be due to the crystalline phase related to Tridymite form of SiO_2 (quartz) with a coherent crystalline domain size of about 4.257 Å [35,36].

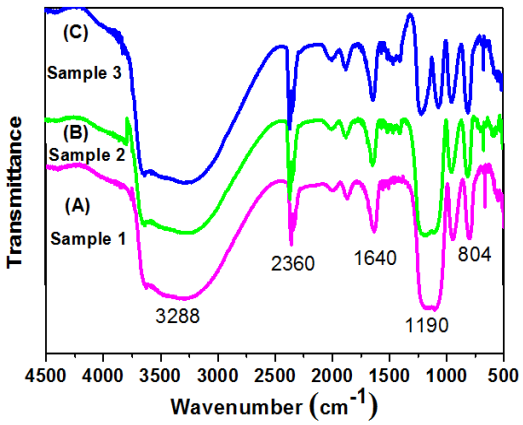

Fig. 2. (A)-(C). FTIR spectrum of Sample 1, 2 and 3

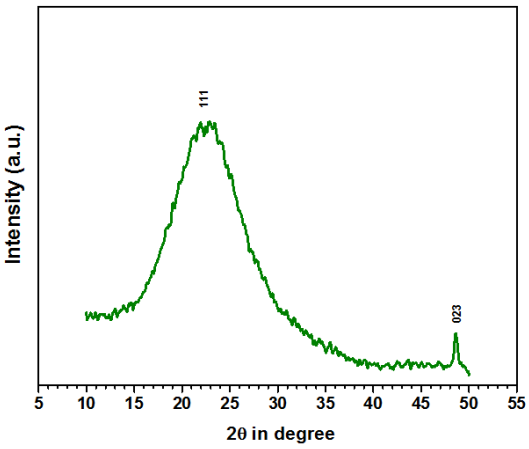

Fig. 3. Powder XRD pattern of SNPs

The SAED images of three samples of SNPs showed bright rings as illustrated in Fig. 4. This may be occurred due to the glass nanoparticles form of the material.

Further, the TEM investigations confirmed the formation of uniform monodispersed, different sizes of SNPs as presented in Fig. 5 (A)-(C). All particles exhibited spherical shape and smooth surface. The TEM images revealed a well-built porous structure. In all the particles, the pores were unwrapped, not well-organized and oriented from the centre to the outer surface. The average particle sizes in sample 1, 2 and 3 were found to be 144.7 nm, 238.34 nm and 291.1 nm, respectively. The different sizes of particles may be explained in terms of kinetic effect of hydrolysis rate of TEOS [29].

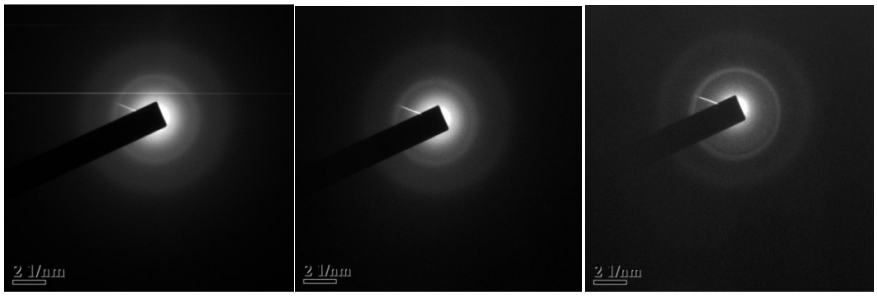

Fig. 4. SAED images of sample 1, 2 and 3

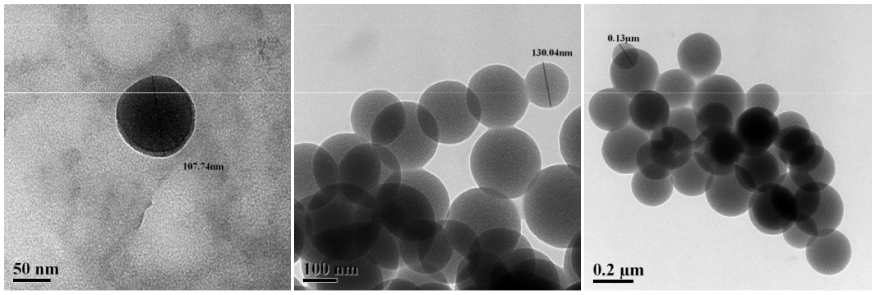

Fig. 5. (A). TEM images of sample 1

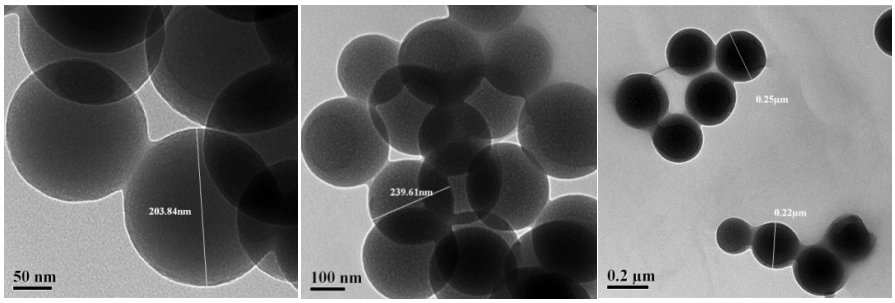

Fig. 5. (B). TEM images of sample 2

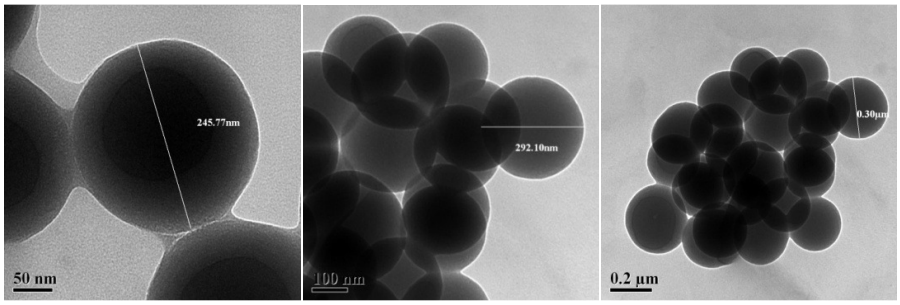

Fig. 5. (C). TEM images of sample 3

The EDX spectra of sample 1 and 2 are presented in Fig. 6. The spectra confirmed the presence of silicon and oxygen in all samples. The average ratio of percentage atomic number for Si and O was found to be 1:2. The spectra also showed the peaks of C and Cu as the experiments were carried out with carbon coated copper grid during sample preparation.

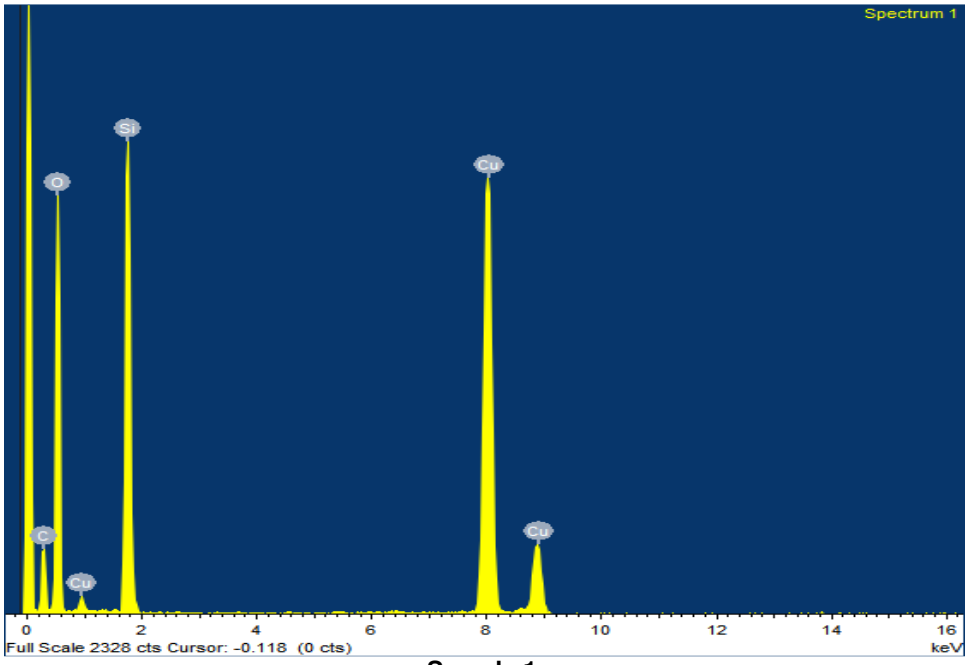

Sample 1

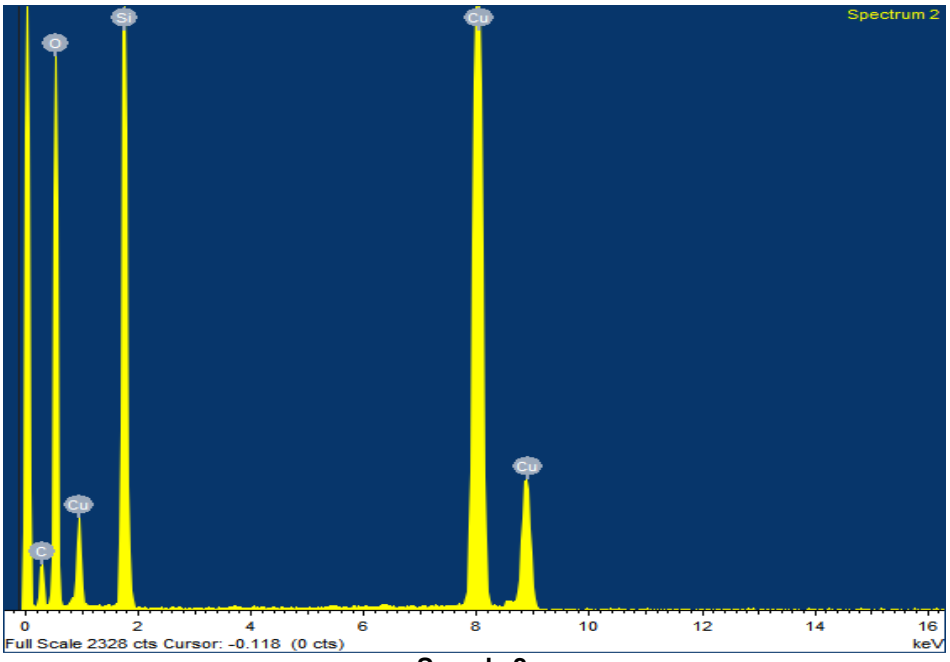

Sample 2

Fig. 6. EDX spectra of sample 1 and 2

The weight losses of Al foils with respect to time in the absence (Fig. 7 A) and presence Fig. 7 B, C, D of SNPs samples in 0.1 M NaOH solution are illustrated in Fig. 7. The corrosion parameters are summarized in Table 1. It could be obvious from Table 1 that IE_W % increases with lowering the particle size of SNPs. The cause of the preferable protection by SNPs may be due to the fact that the surface coverage of Al increases by the adsorption of inhibitor molecules [19]. It may

be assumed that small sized SNPs may block the active site of Al effectively compared to large particles. However, it is clear from the Table 1 that the inhibition efficiencies are slightly elevated. This may be due to the agglomeration effect of nanoparticles for long time intervals [37].

The potentiodynamic polarization curves are shown in Fig. 8 and the corrosion kinetic parameters derived from these curves are represented in Table 2.

The close scrutiny of Fig. 8 and Table 2 revealed that I_{corr} increased noticeably with increase in particle sizes of SNPs from sample 1 to 3; however, the E_{corr} values were shifted towards more negative direction. With the addition of SNPs to 0.1 M NaOH, drastic changes were observed in both the anodic and cathodic parts of the curve. This indicates that the addition of SNPs to alkaline solution suppressed the anodic dissolution of metal as well as cathodic oxygen reduction reaction [38]. The nano particles reduced the rate of cathodic oxygen reduction reactions by blocking oxygen diffusion process. Ultimately, the overall reactions were monitored by the slow cathodic rate determining step. In alkaline solutions silicates form protective layers that slow down the cathodic reaction rate by limiting the diffusion of oxygen to the metal surface causing enhancement of the alkalinity at cathodic sites [39,40]. Therefore, it can be concluded that SNPs in alkaline solution does act as cathodic inhibitor with respect to control solution. The obtained IE_T % values are in agreement with the values of weight loss measurements.

The FE-SEM images of Al immersed in 0.1 M NaOH solution in the absence and presence of sample 1 and 3 are recorded to see the surface morphology of the metal after interactions with SNPs and are presented in Figs. 9 (A)-(C). It is seen from Fig. 9 (A) that the metal surface is strongly scratched in the absence of SNPs and the surface is highly porous. However, in the presence of smaller sized SNPs in Fig. 9 (B), the specimen surface is observed less porous and scratched in more regular way. Fig. 9 (B) is credited to the formation of an improved defensive layer by SNPs compared to Fig. 9 (C). The presence of SNPs onto Al surfaces are further proved by EDX analysis as shown in Figs. 10 (A-B). Hence, the FE-SEM and EDX studies indicate the changes of surface morphology with the rate of corrosion of Al.

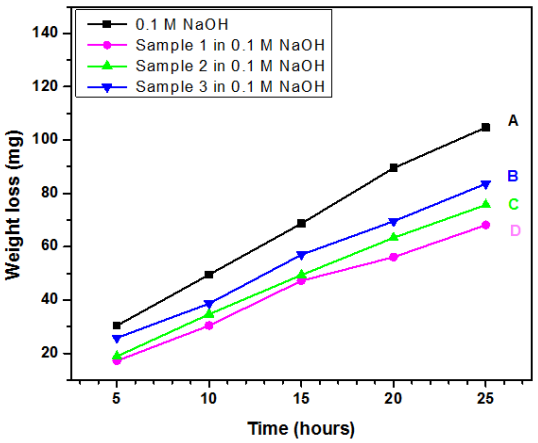

Fig. 7. Weight losses of Al in absence and presence of three SNPs samples in 0.1 M NaOH solution

Table 1. IE_W % obtained from weight loss measurements of Al in 0.1 M NaOH without and with three SNPs sample

Name of the sample	Concentration of NaOH (M)	C_{rate} (mg cm^{-2} h^{-1})	IE_W %
Blank	0.1	1.76	-
Sample 3	0.1	1.39	21
Sample 2	0.1	1.26	28
Sample 1	0.1	1.13	37

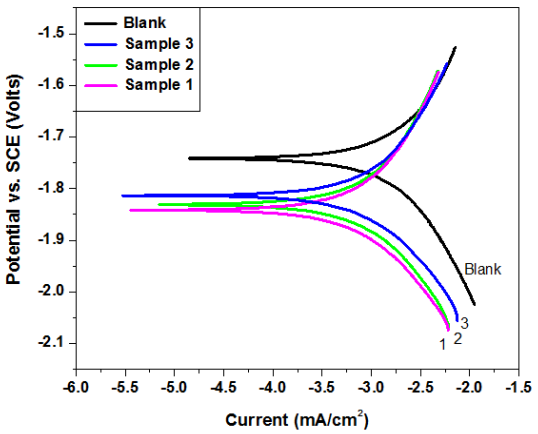

Fig. 8. Polarization curves for Al in 0.1 M NaOH in the absence and presence of three SNPs samples

Table 2. Polarization parameters for Al in 0.1 M NaOH in the absence and presence of three SNPs samples

Name of the Sample	Conc. of NaOH (M)	I_{corr} ($\mu A/cm^2$)	$-E_{corr}$ (mV)	β_a (mV/decade)	β_c (mV/decade)	IE_T %
Blank	0.1	1764	1742	336	340	-
Sample 3	0.1	1108	1820	360	290	37
Sample 2	0.1	927	1837	349	234	48
Sample 1	0.1	776	1849	345	230	56

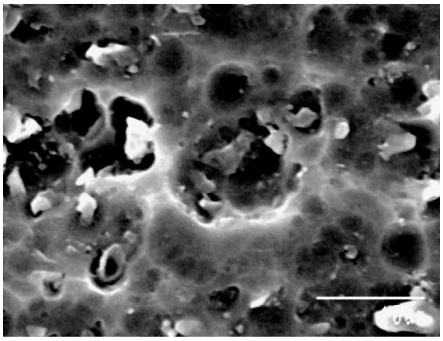

Fig. 9. (A). SEM image of Al metal in 0.1 M NaOH solution

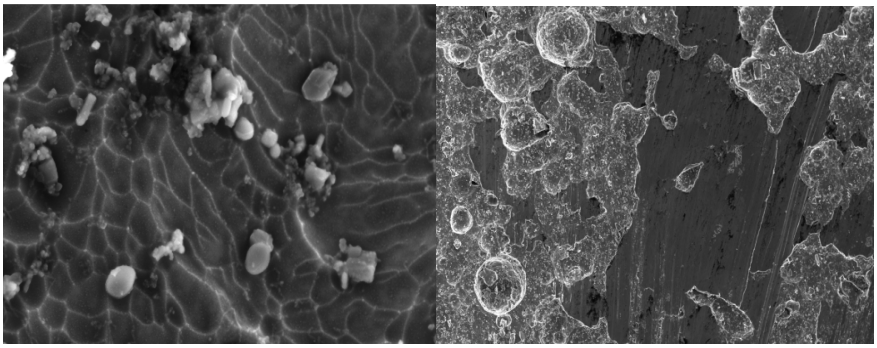

Fig. 9. (B). SEM images of Al metal in 0.1 M NaOH solution of sample 1

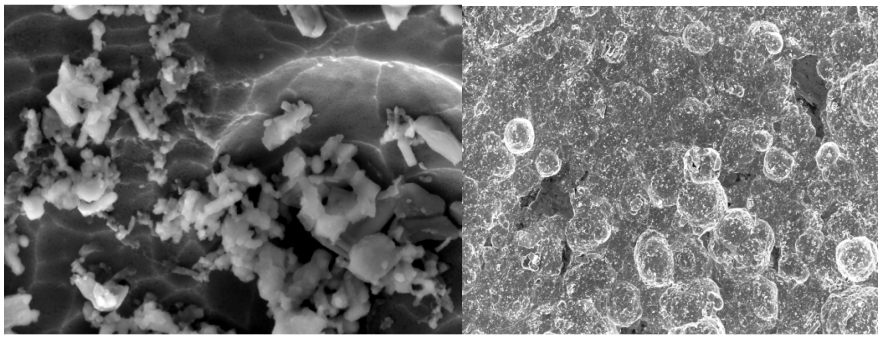

Fig. 9. (C). SEM images of Al metal in 0.1 M NaOH solution of sample 3

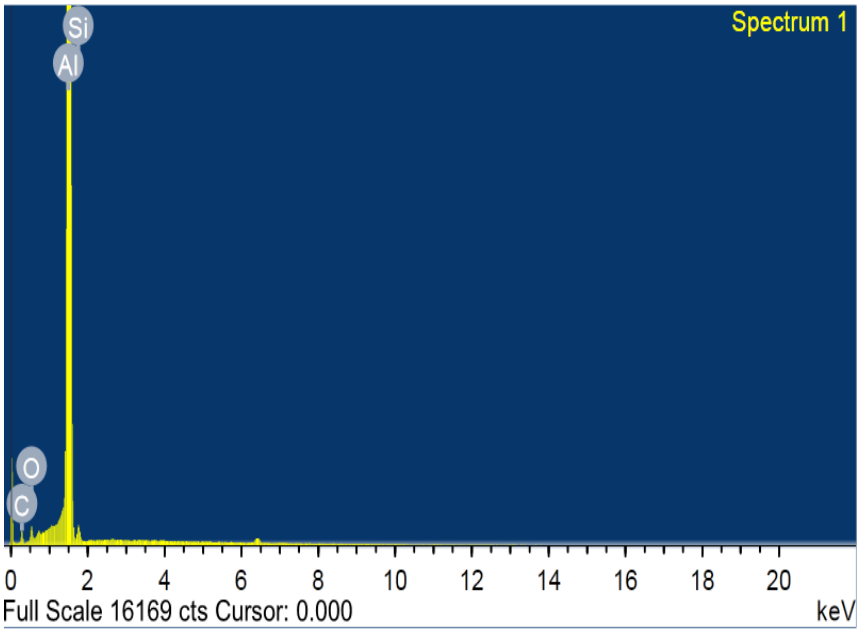

Sample 1

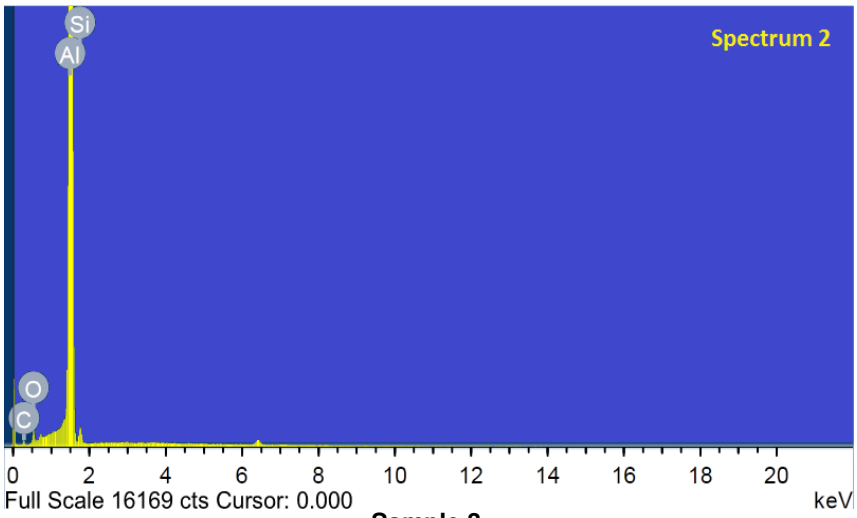

Sample 3

Fig. 10. (A) and (B): EDX of Al in 0.1 M NaOH solution of Sample 1 and 3

Chemical compositions present in sample 1 in Fig. 10 (A).

Elem...	Weight%	Atomic%
C	12.45	23.81
O	2.89	4.16
Al	83.42	71.02
Si	1.24	1.01

Chemical compositions present in sample 3 in Fig. 10 (B).

Elem...	Weight%	Atomic%
C	6.81	13.85
O	2.96	4.52
Al	88.43	80.06
Si	1.80	1.56

The plausible mechanistic pathway for formation of SNPs is shown below.

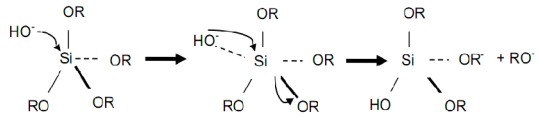

R= - C_2H_5

The weight loss, electrochemical experiment, FE-SEM and EDX studies suggest that Al corrosions are retarded in the presence of SNPs in alkaline medium and it is observed that with lowering of particle sizes, the corrosion protection efficiencies of SNPs onto Al metal surface are found to increase.

Generally, Al corrosion in alkaline medium occurs through two reactions:

(1) Anodic reaction; which leads to metal dissolution.

$$Al \rightarrow Al^{3+} + 3e^- \quad \text{..... (4)}$$

(2) In alkaline solution, the cathodic reaction is typically oxygen reduction.

$$O_2 + 2H_2O + 4e^- \rightarrow 4OH^- \quad \text{..... (5)}$$

It seems that blocking effect of SNPs, which decrease the sizes of the holes during coating and smaller nanoparticles are compatible to the cavities exhibiting greater protection efficacy. Secondly, when smaller size nanoparticles are doped in the film, the cathodic reaction i.e. reduction of oxygen (eqn. 5) is suppressed [19] may be due to decrease of roughness factor. Again, SNPs react with NaOH to form sodium silicate (Na_2SiO_3) and this will form aluminium silicate complex with Al^{+3} ions. This complex probably prevents diffusion of oxygen and retards cathodic reaction.

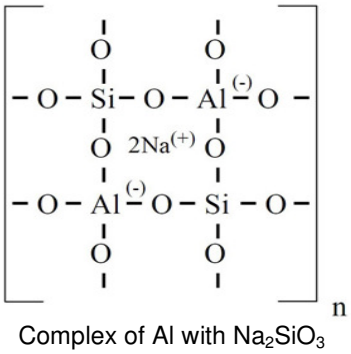

Complex of Al with Na_2SiO_3

4. CONCLUSION

The present study demonstrated that monodispersed, spherical shaped, highly ordered and mesoporous silica nanoparticles (SNPs) can be synthesized by applying an easier aqueous-ethanolic synthetic approach. The particle size was controlled by altering the concentration of tetra-ethoxy silane (TEOS) keeping others parameter unaltered. The potentiodynamic polarization studies revealed that the corrosion protection efficiency of SNPs was increased with decreasing particle size. The corrosion protection efficiency was enhanced by 19% when the average particle size was varied from 291 nm to 144 nm. Moreover, the verification of corrosion inhibition of SNPs onto Al metal in the aforesaid alkaline solution was evident by weight loss studies. The FE-SEM images showed that Al surfaces were less affected in presences of small sized particles.

ACKNOWLEDGEMENTS

The Authors are thankful to Department of Physics, Visva-Bharati University, Santiniketan, India for providing XRD facilities.

COMPETING INTEREST

Authors have declared that no competing interests exist.

REFERENCES

1. Sorkhabia HA, Shabani B, Aligholipour B, Seifzadeh D. The effect of some Schiff bases on the corrosion of aluminium in hydrocholoric acid solution. Applied Surface Science. 2006;252(12):4039-4047.
2. Emregul KC, Abbas AA. The behaviour of aluminium in alkaline medium. Corros Sci. 2000;42(12):2051-2067.
3. Liu Z, Chong PH, Butt AN, Skeldon P, Thompson G. Corrosion mechanism of laser-melted AA 2014 and AA2024 Alloy. Appl. Surf. Sci. 2005;247(1-4):294-299.
4. Tang Y, Lu L, Roesky HW, Wang L, Huang B. The effect of zinc on the aluminum anode of the aluminum–air battery. Journal of Power Sources. 2004;138(1-2):313-318.
5. Egan DR, Leon CPD, Wood RJK, Jones RL, Stokes KR, Walsh FC. Developments in electrode materials and electrolytes for aluminiumeair batteries. Journal of Power Sources. 2013;236:293-310.

6. Clark WJ, Ramsey JD, McCreery RL, Frankel GS. A galvanic corrosion approach to investigating chromate effects on aluminum alloy 2024-T3. J. Electrochem. Soc. 2002;149(5):179-185.
7. Twite RL, Bierwagen GP. Review of alternatives to chromate for corrosion protection of aluminum aerospace alloys. Prog. Org. Coat. 1998;33(2):91-100.
8. El-Naggar MM. Corrosion inhibition of mild steel in acidic medium by some sulpha drugs compounds. Corrosion Sci. 2007;49(5):2226-2236.
9. Borisova D, Mohwald H, Shchukin DG. Mesoporous silica nanoparticles for active corrosion protection. Acs Nano. 2011;5(3):1939-1946.
10. Van Ooij WJ, Zhu DQ, Prasad G, Jayaseelan S, Fu Y, Teredesai N. Silane based chromate replacements for corrosion control, paint adhesion, and rubber bonding. Surf. Eng. 2000;16(5):386-396.
11. Zheludkevich ML, Serra R, Montemor MF, Yasakau KA, Salvado IMM, Ferreira MGS. Nanostructured sol–gel coatings doped with cerium nitrate as pre-treatments for AA2024-T3 Corrosion protection performance. Electrochim. Acta. 2005;51(2):208-217.
12. Zheludkevich ML, Serra R, Montemor MF, Salvado IMM, Ferrreira MGS. Corrosion protective properties of nanostructured sol–gel hybrid coatings to AA2024-T3. Surf. Coat. Technol. 2006;200(9):3084-3094.
13. Brusciotti F, Batan A, Graeve ID, Wenkin M, Biessemans M, Willem R, Reniers F, Pireaux JJ, Piens M, Vereecken J, Terryn H. Characterization of thin water-based silane pre-treatments on aluminium with the incorporation of nano-dispersed CeO_2 particles. Surf. Coat. Technol. 2010;205(2):603-613.
14. Palomino LM, Suegama PH, Aoki IV, Montemor MF, Melo HG. Electrochemical study of modified non-functional bis-silane layers on Al alloy 2024–T3. Corros. Sci. 2008;50(5):1258-1266.
15. Rosero-Navarro NC, Pellice SA, Duran A, Aparicio M. Effects of Ce containing sol–gel coatings reinforced with SiO2 nanoparticles on the protection of AA2024. Corros. Sci. 2008;50(5):1283-1291.
16. Moutarlier V, Neveu B, Gidandet MP. Evolution of corrosion protection for sol–gel coatings doped with inorganic inhibitors. Surf. Coat. Technol. 2007;202(10):2052–2058.
17. Quinet M, Neveu B, Moutarlier V, Audebert P, Ricq L. Corrosion protection of sol–gel coatings doped with an organic corrosion inhibitor: Chloranil. Prog. Org. Coat. 2007;58(1):46-53.
18. Raps D, Hack T, Wehr J, Zheludkevich ML, Bastos AC, Ferreira MGS, Nuyken O. Electrochemical study of inhibitor-containing organic–inorganic hybrid coatings on AA2024. Corros. Sci. 2009;51(5):1012-1021
19. Dalmor V, Dos Santos JHZ, Armelin E, Aleman C, Azambuja DS. Phosphonic acid/silica-based films: A potential treatment for corrosion protection. Corr. Sci. 2012;60:173-180.
20. Magda AA, Hesham FA, Hesham MAS, Aref MEAbER, Ahmed IAE. Preparation and Characterization of Silica Nanoparticles by Wet Mechanical Attrition of White and Yellow Sand. J Nanomed and Nanotechnol. 2013;4(6). Available: http://dx.doi.org/10.4172/2157-7439.1000183.
21. Anna BC, Federica B, Anna MF, Bonaventura F, Cristina L. Synthesis of silica nanoparticles in a continuous-flow microwave reactor. Powder Technology. 2006;167(1):45-48.
22. Boguch GH, Tracy MA, Zukoski CF. Preparation of monodisperse silica particles: Control of size and mass fraction. J Non-Crystalline Solids. 1988;104(1):95-106.
23. Stanleya R, Nesarajb AS. Effect of surfactants on the wet chemical synthesis of silica nanoparticles. International Journal of Applied Science and Engineering. 2014;12(1):9-21.
24. Zaky RR, Hessien MM, El-Midany AA, Khedr MH, Abdel-Aal EA. Preparation of silica nanoparticles from semi-burned rice straw ash. Powder Techn. 2008;185(1):31-35.
25. Zhao M, Zheng LL, Bai X, Li N, Yu L. Fabrication of silica nanoparticles and hollow spheres using ionic liquid microemulsion droplets as templates. Colloids and Surfaces A: Physicochem. Eng. Aspects. 2009;346(1-3):229-236.
26. Gao GM, Zou HF, Gan SC, Liu ZJ, An BC, XU JJ, Huan Li G. Preparation and properties of silica nanoparticles from oil shale ash. Powder Techn. 2009;191(1-2):47-51.

27. Hee DJ. Experimental study of synthesis of silica nanoparticles by a bench-scale diffusion flame reactor. Powder Techn. 2001;119(2-3):102-108.
28. Patil A, Chirmade UN, Trivedi V, Lamprou DA, Urquhart A, Douroumis D. Encapsulation of water insoluble drugs in mesoporous silica nanoparticles using supercritical carbon dioxide. J Nanomed & Nanotechnol. 2011;2(3):111.
29. Rao KS, Khalil E, Tsutomu K, Kazumi M, Keisuke M. A novel method for synthesis of silica nanoparticles. J Colloid Interf. Sci. 2005;289(1):125–131.
30. Yim H, Kent MS, Tallant DR, Garcia MJ, Majewski J. Hygrothermal degradation of (3-glycidoxypropyl) trimethoxysilane films studied by neutron and X-ray reflectivity and attenuated total reflection infrared spectroscopy. Langmuir. 2005;21(10): 4382-4392.
31. Franquet A, Terryn H, Vereecken J. Composition and thickness of non-functional organosilane films coated on aluminium studied by means of infrared spectroscopic ellipsometry. Thin Solid Films. 2003;441(1-2):76-84.
32. Yazdimamaghani M, Pourvala T, Motamedi E, Fathi, B, Vashaee D and Tayebi L. Synthesis and characterization of encapsulated nanosilica particles with an acrylic copolymer by in sit emulsion polymerization using thermoresponsive nonionic surfactant. Materials. 2013;6(9): 3737-3741.
33. Colthup NB, Daly LH, Wiberley SE. Introduction to Infrared and Raman Spectroscopy, second ed., Academic Press, London; 1975.
34. Vansant EF, Voort PV, Vrancken KC. Characterization and chemical modification of silica surface. Studies in surface science and catalysis. Elsevier Science B.V. 1995;93.
35. Bahari H, Aziz SHA, Kamari HM, Yunus WMM, Adikan FRM. The effect of bismuth on the structure and mechanical properties of GeO2–PbO–Bi2O3 ternary bulk glass system. 2012;120(7):280-285.
36. Morris MC, et al. Std. X-ray diffraction powdered patterns section 18-data for 58 substances. International Centre for Diffraction Data. U.S. dept. Of commerce, national bureau of Standards, C 13.44: 25/ sec 18; 1981.
37. Shi X, Nguyen TA, Suo Z, Liu Y, Avci R. Effect of nanoparticles on the anticorrosion and mechanical properties of epoxy coating. Surface & Coatings Technology. 2009;204:237–245.
38. Lebrini M, Robert F, Blandinieres P, Roos AC. Corrosion inhibition by *Isertia coccinea* plant extract in hydrochloric acid solution. Int. J. Electrochem. Sci. 2011;6(7): 2443–2460.
39. Li W, He Q, Zhang S, Pei B, Hou B. Some new triazole derivatives as inhibitors for mild steel corrosion in acidic medium. J. Appl. Electrochem. 2008;38(3):289–295.
40. Papavinasam S. Corrosion Inhibitors. Uhlig's corrosion Handbook, second edition. ISBN 0-471-15777-5. 2000;1089-1105.

Peer-review history:
The peer review history for this paper can be accessed here:
http://www.sciencedomain.org/review-history.php?iid=713&id=5&aid=6581